Application of Shannon's Entropy to Classify Emergent Behaviors in a Simulation of Laser Dynamics

J. L. GUISADO
Centro Universitario de Mérida
Universidad de Extremadura
06800 Mérida (Badajoz), Spain
jlguisado@unex.es

F. JIMÉNEZ-MORALES
Departamento de Física de la Materia Condensada
Universidad de Sevilla
P.O. Box 1065, 41080 Sevilla, Spain
jimenez@us.es

J. M. GUERRA
Departamento de Optica, Facultad de CC. Físicas
Universidad Complutense de Madrid
28040 Madrid, Spain
jmguerra@fis.ucm.es

Abstract—Laser dynamics simulations have been carried out using a cellular automata model. The Shannon's entropy has been used to study the different emergent behaviors exhibited by the system, mainly the laser spiking and the laser constant operation. It is also shown that the Shannon's entropy of the distribution of the populations of photons and electrons reproduces the laser stability curve, in agreement with the theoretical predictions from the laser rate equations and with the experimental results.

Keywords—Computational physics, Parallel modelling and simulation, Cellular automata, Complex systems, Laser physics.

1. INTRODUCTION

Laser dynamics has been traditionally analyzed by solving a set of coupled differential rate equations which describe the interrelationships and transition rates among the electronic states in the laser active medium and the laser photons [1,2]. But recently, an alternative approach based

Partially supported by the Junta de Extremadura (Consejería de Educación, Ciencia y Tecnología) and the European Social Fund, Grant MOV03B170.

on a cellular automata (CA) model has been proposed [3], in which the laser properties arise as emergent phenomena from the collective effect of many locally interacting, simple components. In this paper we focus on the application of Shannon's entropy to recognize and classify the different types of behavior shown by the CA model.

Cellular automata are a class of spatially and temporally discrete mathematical systems, characterized by local interaction and synchronous dynamical evolution. They were first introduced in the 1950s by von Neumann [4] to investigate self-reproduction and since then have attracted much interest because of its capability to generate complex behavior from sets of components which interact locally with relatively simple rules [5,6]. In the last two decades, CA have been extensively used to build models of a wide variety of physical systems [7,8], for example reaction-diffusion processes [9], fluid dynamics [10], magnetization in solids [11], growth phenomena [12], molecular excited-state dynamics [13], etc. Recently, CA have become more attractive because the inherent parallelism makes them very suitable to be naturally and efficiently implemented in parallel computers. High performance simulations of physical systems [14,15] can be carried out in this way.

A laser cellular automata model can be useful for two kinds of application: first, for cases in which the standard treatment cannot be applied—as happens in lasers governed by stiff differential equations, with convergence problems—second, to take advantage of the cellular automata intrinsic parallel nature in order to efficiently implement three-dimensional simulations of laser devices in parallel computers.

In this work, we study the following problem. In the laser cellular automata model, laser field and population inversion may perform different kinds of temporal behavior, depending on the values of the pumping probability, the life time of laser photons, and the upper laser level life time. The problem is how to find a magnitude to characterize all these possible outcomes of the system to be compared with the predictions of the traditional approach for laser dynamics (the laser rate equations) and with the experimental results.

In order to address this problem, we choose the Shannon's entropy as such magnitude. In the laser CA model, two main kinds of temporal behavior are found: an overdamped dynamics with almost null Shannon's entropy and an oscillating one with larger Shannon's entropy. With the Shannon's entropy, we locate these different kinds of behavior and check the agreement between the laser CA model results and the predictions of the laser rate equations.

This paper is organized as follows. Section 2 describes the cellular automata model that has been used for the simulations. In Section 3, the results of the simulations are presented and analyzed using the Shannon's entropy. Finally, the conclusions are summarized in Section 4.

2. CELLULAR AUTOMATA MODEL

The model that has been used is a cellular automaton defined on a two-dimensional square lattice of $N_c = 200 \times 200$ cells with periodic boundary conditions. Two variables $a_i(t)$ and $c_i(t)$ are associated to each node of this lattice. The first one, $a_i(t)$, represents the state of the electron in node i at a given time t. An electron in the laser ground state takes the value $a_i(t) = 0$, while an electron in the upper laser state takes the value $a_i(t) = 1$. The second variable $c_i(t) \in \{0, 1, 2, \ldots, M\}$ represents the number of photons in node i at time t. A large enough upper value of M is taken to avoid saturation of the system. The neighborhood considered is the *Moore neighborhood*, each cell having nine neighbors: the cell itself, its four nearest neighbors (situated in the positions north, south, east, and west) and the four next neighbors (in the positions northeast, southeast, northwest and southwest). The time evolution of the CA is given by a set of transition rules which determine the state of any particular cell of the system at time $t + 1$ depending on the state of the cells included in its neighborhood at time t. These rules represent the different physical processes that work at the microscopic level in a laser system.

R1. Pumping: If the electronic state of a cell has a value of $a_i(t) = 0$ in time t, then in time $t + 1$ that state will have a value of $a_i(t + 1) = 1$ with a probability λ.

R2. Stimulated Emission: If, in time t, the electronic state of a cell has a value of $a_i(t) = 1$ and the sum of the values of the laser photons states in the nine neighbor cells is greater than a certain threshold (which in our simulations has been taken to be 1), then in time $t + 1$ a new photon will be created in that cell: $c_i(t + 1) = c_i(t) + 1$ and the electron will decay to the ground level: $a_i(t + 1) = 0$.

R3. Photon Decay: A finite life time τ_c is assigned to each photon when it is created. The photon will be destroyed τ_c time steps after it is created.

R4. Electron Decay: A finite life time τ_a is assigned to each electron that is promoted from the ground level to the upper laser level. That electron will decay to the ground level again τ_a time steps after it was promoted, if it has not yet decayed by stimulated emission. To simplify the model as much as possible, we consider this decay is entirely nonradiative, i.e., we do not take into account spontaneous emission. Also, as in an ideal four level laser the population of level E_1 is negligible, stimulated absorption has not been considered.

In addition, a small continuous noise level of random photons in the laser mode is introduced at every time step, in order to represent the experimentally observed noise level, responsible of the initial laser start-up. This is done by making $c_i(t + 1) = c_i(t) + 1$ for a small number of cells ($< 0.01\%$ of total) with randomly chosen positions.

3. SIMULATION RESULTS AND SHANNON'S ENTROPY ANALYSIS

Three parameters determine the response of the system: the pumping probability (λ), the life time of photons (τ_c) and the life time of excited electrons (τ_a). Initially, $a_i(0) = 0$, $c_i(0) = 0$, $\forall i$, except a small fraction 0.01% of noise photons. We let the system evolve for 500 time steps. In each time step, the total number of laser photons $n(t) = \sum_{i=1}^{N_c} c_i(t)$, and the total number of electrons in the upper laser state (population inversion) $N(t) = \sum_{i=1}^{N_c} a_i(t)$ are measured.

Running test simulations for different values of the three parameters of the system, two main types of behavior are observed: after a transient time, $n(t)$ and $N(t)$ show either a constant value or correlated damped oscillations. We are interested in making a more systematic exploration of the behavior of the laser CA model in the whole parameters space, and comparing it with the response of the laser rate equations.

To this end, it should be interesting to find a magnitude to characterize the type of behavior shown by the system for each particular triad of values of the parameters. As such a magnitude, the Shannon's entropy S of the distribution of values taken by $n(t)$ and $N(t)$, after running the simulation for a time interval, is calculated. This Shannon's entropy is computed by dividing the range of values taken by n or N in 10^3 equally spaced bins, and computing the frequency (f_i) at which this value lies inside every particular nonvoid bin i. Then, S is calculated as

$$S(\lambda, \tau_c, \tau_a) = -\sum_{i=1}^{m} f_i \log_2 f_i, \tag{1}$$

where m is the number of nonvoid bins.

The Shannon's entropy S measures the dispersion of the distribution of values taken by the number of laser photons n (or the population inversion N). If this number is approximately constant (i.e., all the bins except one are void), S will tend to zero; if oscillations appear, the probability distribution becomes wider and S takes higher values; and finally the maximum value of S would result from an equiprobable distribution. Therefore, S can be used as a good indicator of the presence of oscillations in the system. The dependence of the Shannon's entropy on two of

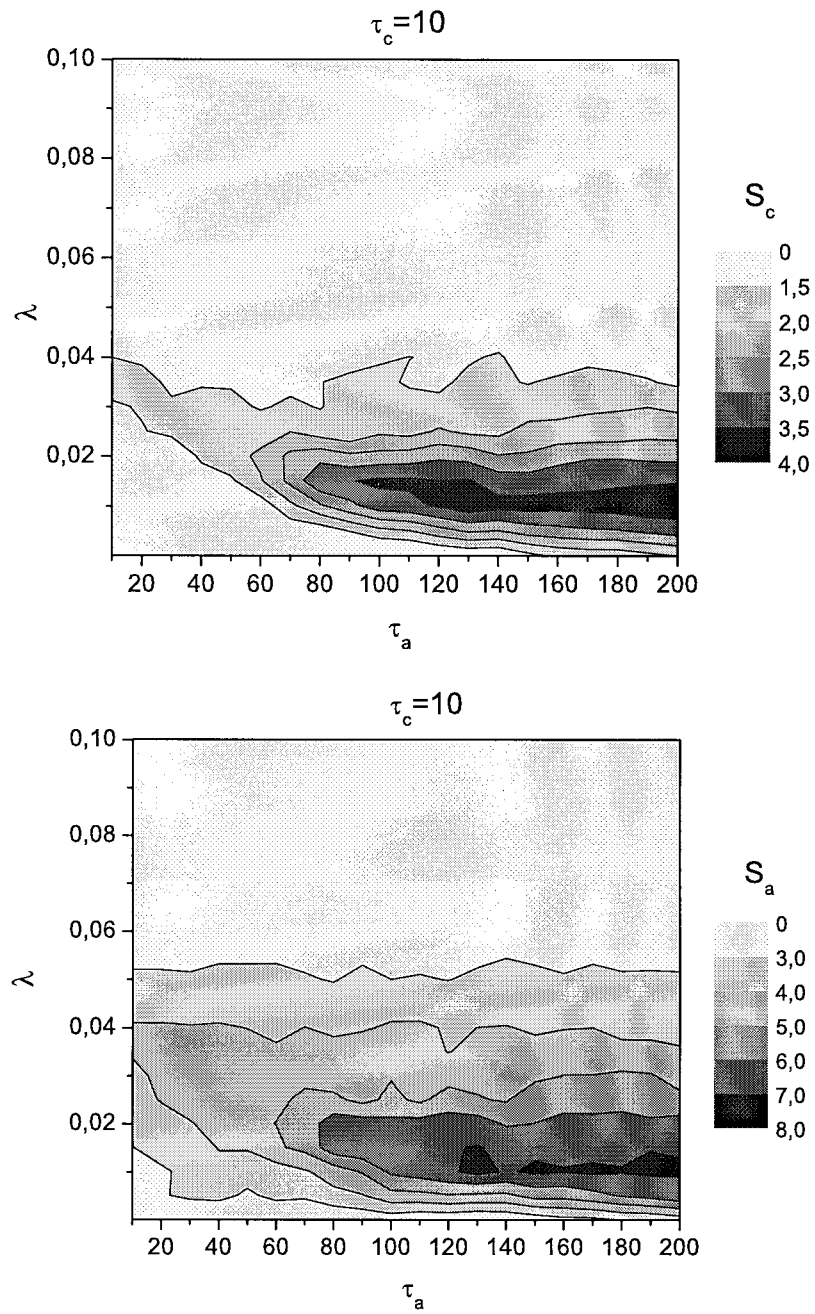

Figure 1. Contour plots of the Shannon's entropy of the distribution of values taken by the number of laser photons S_c (top) and the population inversion S_a (bottom), showing the dependence of S with the pumping probability λ and the upper laser level life time τ_a for a fixed value of the cavity life time of $\tau_c = 10$. τ_a and τ_c are measured in time steps. S has been computed for a period of time: $t \in [250, 1000]$ time steps.

the parameters of the system when the third parameter is fixed is shown in Figure 1. Similar plots can be obtained for other values of the parameter that is fixed (τ_c), showing areas in which S tends to zero, indicating a constant behavior (bright zones), and other areas in which S is higher, indicating an oscillatory behavior (dark zones).

The results obtained by measuring S can be compared with the predictions of the laser rate equations for a wide range of values of the three parameters of the system. The laser rate equations can be put in their simplest—but still meaningful—form as a system of two coupled

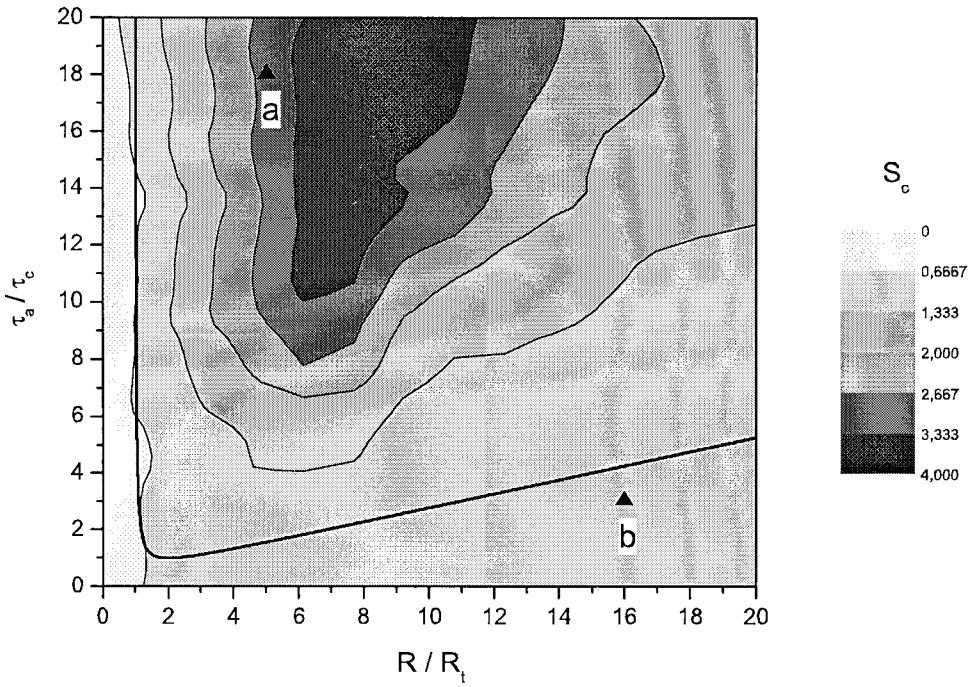

Figure 2. Contour plot of the Shannon's entropy of the distribution of the number of laser photons for a fixed value of $\tau_c = 10$ time steps. Low values of S_c (bright zones) indicate that the response of the system is nonoscillatory, while high values (dark zones) correspond to an oscillatory response. The black line is the theoretical stability curve. Points a and b correspond to the parameters for which the temporal evolution is shown in Figure 3. (a): $R/R_t = 5$, $\tau_a/\tau_c = 18$. (b): $R/R_t = 16$, $\tau_a/\tau_c = 3$.

differential equations [1,2]. The first one gives the variation with time of the number of laser photons $n(t)$ and the other one reflects the temporal variation of the population inversion $N(t)$,

$$\frac{dn(t)}{dt} = K\,N(t)\,n(t) - \frac{n(t)}{\tau_c}, \tag{2}$$

$$\frac{dN(t)}{dt} = R - \frac{N(t)}{\tau_a} - K\,N(t)\,n(t). \tag{3}$$

Here, R is the pumping rate and K is a constant called "coupling constant". For the case of small amplitude fluctuations, a linearized small-signal analysis of these equations can be carried out, and two different situations arise.

1. Overdamped System: The solutions for $n(t)$ and $N(t)$ are real exponentials. The response to any perturbation dies out exponentially towards the steady state.
2. Relaxation Oscillations: The solutions have an exponentially damped sinusoidal form. The response to any perturbation shows relaxation oscillations towards the steady state, with a frequency (usually called *spiking frequency*),

$$\omega_{sp} = \sqrt{\left(\frac{1}{2\,\tau_a}\frac{R}{R_t}\right)^2 - \frac{1}{\tau_a\,\tau_c}\left(\frac{R}{R_t} - 1\right)}. \tag{4}$$

Here, R is the laser pumping rate and R_t is the threshold laser pumping rate, which are linearly related to the pumping probability λ and the threshold pumping probability λ_t that appear in the CA model [3], so that $R/R_t = \lambda/\lambda_t$. The threshold pumping probability λ_t is calculated in the CA model as the smallest value of the pumping probability λ for which after a transient time the number of laser photons is clearly greater than the number of noise photons introduced.

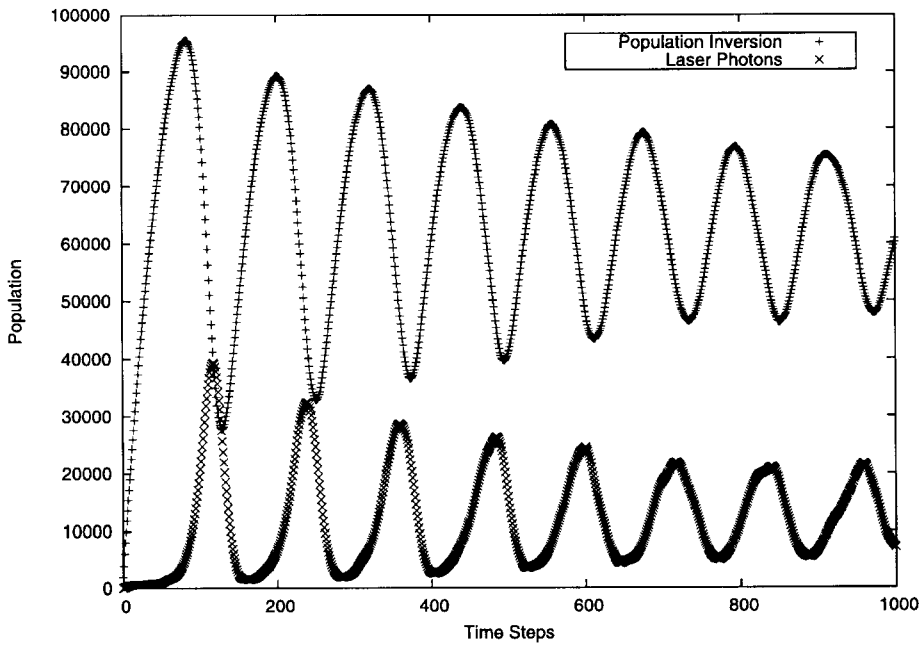

(a)

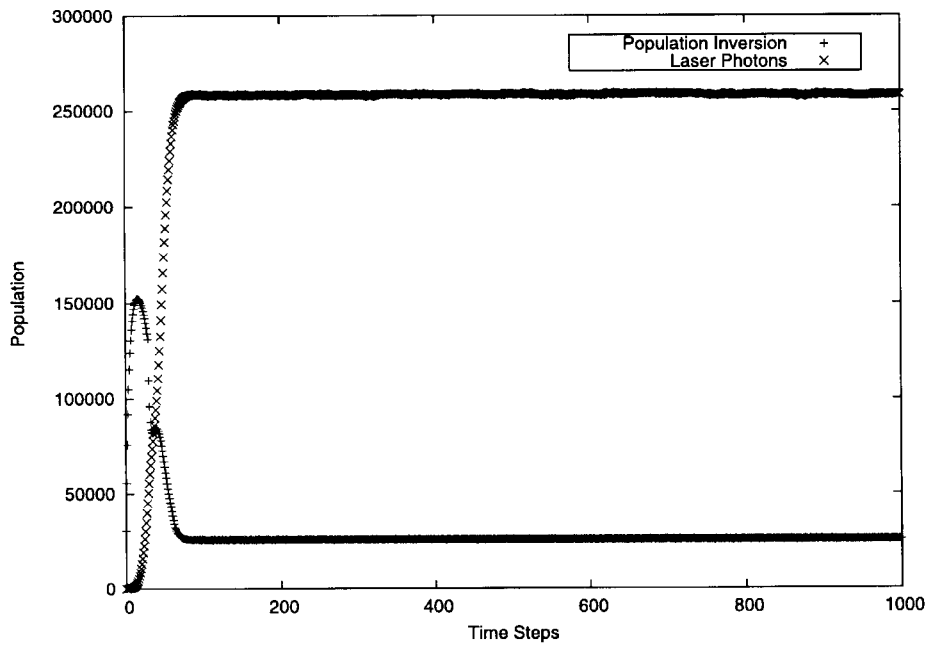

(b)

Figure 3. Temporal evolution of the system (number of laser photons and population inversion) for the values of the parameters marked as a and b points in Figure 2. The values of the parameters are (a): $\lambda = 0.0125$, $\tau_c = 10$, $\tau_a = 180$. (b): $\lambda = 0.192$, $\tau_c = 10$, $\tau_a = 30$. Here, τ_c and τ_a are measured in time steps. Lattice: 400 × 400 cells.

The necessary condition for the occurrence of the relaxation oscillations is that ω_{sp} be real, or equivalently, that the quantity inside the square root in equation (4) be positive. This leads to the following condition,

$$\frac{\tau_a}{\tau_c} > \frac{(R/R_t)^2}{4\,(R/R_t - 1)}. \tag{5}$$

Damped oscillations appear for values of the parameters fulfilling condition (5), and a constant behavior appears if this condition is not satisfied. The values of the parameters for which these two situations appear can be visualized by plotting the equation derived from condition (5) with an equal sign, using R/R_t as x-axis and τ_a/τ_c as y-axis. The result is the black line in Figure 2. This function is the *theoretical stability curve* which separates areas of different behavior for the solution of the linearized small-signal laser rate equations: relaxation oscillations appear above and to the right of this curve and an overdamped behavior below and to the left of it.

In order to compare the behavior exhibited by the results of the laser cellular automata model with these predictions from the laser rate equations, we have plotted in the same graph in Figure 2, the Shannon's entropy for the number of laser photons, using R/R_t as x-axis and τ_a/τ_c as y-axis. It can be observed that the Shannon's entropy follows the form of the theoretical stability curve. Areas of high S (dark zones)—which indicate an oscillatory behavior in the results of the laser CA model—appear above and to the right of this curve, and areas of low S (bright zones)—which indicate a constant behavior in the results of the laser CA model—appear below and to the left of it. This is in agreement with the solutions of the laser rate equations.

Figure 3 shows the time evolution of $n(t)$ and $N(t)$ corresponding to the points a and b in Figure 2. Relaxation oscillations (also known as *laser spiking*) are found for point a, included in the zone of high entropy, and a constant behavior for point b, included in the zone of low entropy.

The information obtained by the Shannon's entropy not only is in agreement with the results of the laser rate equations, but is richer than that obtained only from the stability analysis of those equations, because it is able to quantify the amplitude of the oscillatory behavior. Therefore, the Shannon's entropy can be used as a parameter to characterize the behavior exhibited by the laser CA model and to compare it with the dynamics predicted by the laser rate equations.

4. CONCLUSIONS

Along this paper it was shown the usefulness of the Shannon's entropy concept to test the agreement between the different behaviors observed in the laser cellular automata model with those predicted by the stability analysis performed in the laser rate equations. This agreement reinforces the confidence in the capability of laser cellular automata as a modelling tool—alternative to differential equations—to describe laser physics.

REFERENCES

1. A.E. Siegman, *Lasers*, University Science Books, (1986).
2. O. Svelto, *Principles of Lasers*, Plenum Press, (1989).
3. J.L. Guisado, F. Jiménez-Morales and J.M. Guerra, A cellular automaton model for the simulation of laser dynamics, *Phys. Rev. E* **67:066708**, (2003).
4. J. von Neumann, *Theory of Self-Reproducing Automata*, University of Illinois Press, Urbana, IL, (1966).
5. S. Wolfram, Universality and complexity in cellular automata, *Physica D* **10** (1), (1984).
6. S. Wolfram, *Cellular Automata and Complexity*, Addison-Wesley, (1994).
7. B. Chopard and M. Droz, *Cellular Automata Modelling of Physical Systems*, Cambridge University Press, (1998).
8. T. Toffoli and N. Margolus, *Cellular Automata Machines: A New Environment for Modelling*, The MIT Press, (1987).
9. B. Chopard, P. Luthi and M. Droz, Reaction-diffusion cellular automata model for the formation of Liesegang patterns, *Phys. Rev. Lett.* **72** (9), 1384–1387, (1994).
10. A.K. Gunstensen, D.H. Rothman, S. Zaleski and G. Zanetti, Lattice Boltzmann model of inmiscible fluids, *Phys. Rev. A* **43**, 4320–4327, (1991).
11. G. Vichniac, Simulating physics with cellular automata, *Physica D* **10**, 96–115, (1984).
12. J. Gravner and D. Griffeath, Cellular automaton growth on Z^2: Theorems, examples and problems, *Adv. Appl. Math.* **21**, 241–304, (1998).
13. P.G. Seybold, L.B. Kier and C.-K. Cheng, Aurora borealis: Stochastic cellular automata simulations of the excited-state dynamics of oxygen atoms, *Int. J. Quant. Chem.* **75**, 751–756, (1999).

14. P.M.A. Sloot, J.A. Kaandorp, A.G. Hoekstra and B.J. Overeinder, Distributed simulation with cellular automata: Architecture and applications, In *SOFSEM'99: Theory and Practice of Informatics, Lecture Notes on Computer Science, Volume 1725*, (Edited by J. Pavelka, G. Tel and M. Bartošek), pp. 203–248, (1999).
15. D. Talia, Cellular processing tools for high-performance simulation, *IEEE Computer* **33** (9), 44–52, (September 2000).